Impact of time delays on oscillatory dynamics of interlinked positive and negative feedback loops

Bo Huang, Xinyu Tian, Feng Liu,* and Wei Wang
National Laboratory of Solid State Microstructures, Department of Physics, and Collaborative Innovation Center of Advanced Microstructures, Nanjing University, Nanjing 210093, China
(Received 8 June 2016; published 28 November 2016)

Interlinking a positive feedback loop (PFL) with a negative feedback loop (NFL) constitutes a typical motif in genetic networks, performing various functions in cell signaling. How time delay in feedback regulation affects the dynamics of such systems still remains unclear. Here, we investigate three systems of interlinked PFL and NFL with time delays: a synthetic genetic oscillator, a three-node circuit, and a simplified single-node model. The stability of steady states and the routes to oscillation in the single-node model are analyzed in detail. The amplitude and period of oscillations vary with a pointwise periodicity over a range of time delay. Larger-amplitude oscillations can be induced when the PFL has an appropriately long delay, in comparison with the PFL with no delay or short delay; this conclusion holds true for all the three systems. We unravel the underlying mechanism for the above effects via analytical derivation under a limiting condition. We also develop a stochastic algorithm for simulating a single reaction with two delays and show that robust oscillations can be maintained by the PFL with a properly long delay in the single-node system. This work presents an effective method for constructing robust large-amplitude oscillators and interprets why similar circuit architectures are engaged in timekeeping systems such as circadian clocks.

DOI: 10.1103/PhysRevE.94.052413

I. INTRODUCTION

The design principle for genetic oscillators has been a focus of research in the fields of systems and synthetic biology. Robust oscillation is essential for accurate timing of cellular periodic behaviors such as circadian rhythms [1] and the cell cycle [2]. The understanding of those natural oscillating systems has provided insights into the construction of robust oscillators. For example, negative feedback is indispensable for oscillation [3]; however, a negative feedback loop (NFL) alone is often insufficient for reliable oscillation due to its weak robustness against cellular noise [4,5]. In contrast, interlinking a positive feedback loop (PFL) with an NFL can contribute to the robustness and tunability of oscillation [5–8].

Since feedback loops in biological systems usually involve multiple intermediate processes such as transcription, translation, transport between the nucleus and cytoplasm, and posttranslational modifications [7,9], time delays are inevitable in feedback regulation. The effect of delayed negative feedback on oscillatory dynamics has been probed widely [3]. Interlinking delayed NFLs allows for a variety of behaviors including complex periodic, aperiodic, and chaotic dynamics [10,11], as well as frequency locking, phase drift, and amplitude death [12].

Time delays can remarkably affect the role for additional PFLs in modulating oscillation. A PFL with no delay or a short delay, separately called nPFL and sPFL for short, may facilitate the induction of oscillation and increase its robustness [7,8,13]. Conversely, a PFL with a delay comparable to that of an NFL may go against robust oscillation [7]. However, whether a PFL with a long delay, called lPFL, plays a constructive role remains open, although it was briefly mentioned that an lPFL can induce oscillations [14]. Strikingly, the PFLs in circadian clocks of *Neurospora crassa*, *Drosophila*, and mammals seem to involve more time-consuming processes like transcription or translation than the accompanying NFLs [15–21]. Thus, it is essential to unravel a full spectrum of influence of the delayed PFL on oscillatory dynamics.

To this end, we systematically investigate the role for delayed PFL in modulating oscillation and explore the underlying mechanisms. This paper is organized as follows. In Sec. II, we revisit a mathematical model of a synthetic genetic circuit and show that the PFL with a properly long delay can help induce larger-amplitude oscillations than the nondelayed PFL, the generality of which is further tested in a three-node dual-loop model and a simplified one-node model. In Sec. III, we probe how delay time influences Hopf bifurcation and the stability of steady states in the simplified model with multiplicative coupling. In Sec. IV, we systematically investigate the effects of delays on oscillatory dynamics. In Sec. V, the dependence of oscillation amplitude on the delay is analytically derived under a limiting condition. In Sec. VI, we perform stochastic simulations to explore how the robustness of oscillation depends on the delay time. We summarize the main results and discuss their implications in Sec. VII.

II. THREE MODELS AND AN OVERVIEW OF CIRCUIT DYNAMICS

First, we revisit a mathematical model of a synthetic genetic circuit constructed in *Escherichia coli* [5,22,23]. The circuit comprises the genes of an activator (*araC*), a repressor (*lacI*), and a reporter (*yemGFP*, denoted by X for short), which are under the control of the same hybrid promoter $p_{lac/ara-1}$ [Fig. 1(a)]. The activator (repressor) can promote (inhibit) the transcription of three genes by binding to the promoter. The

*fliu@nju.edu.cn

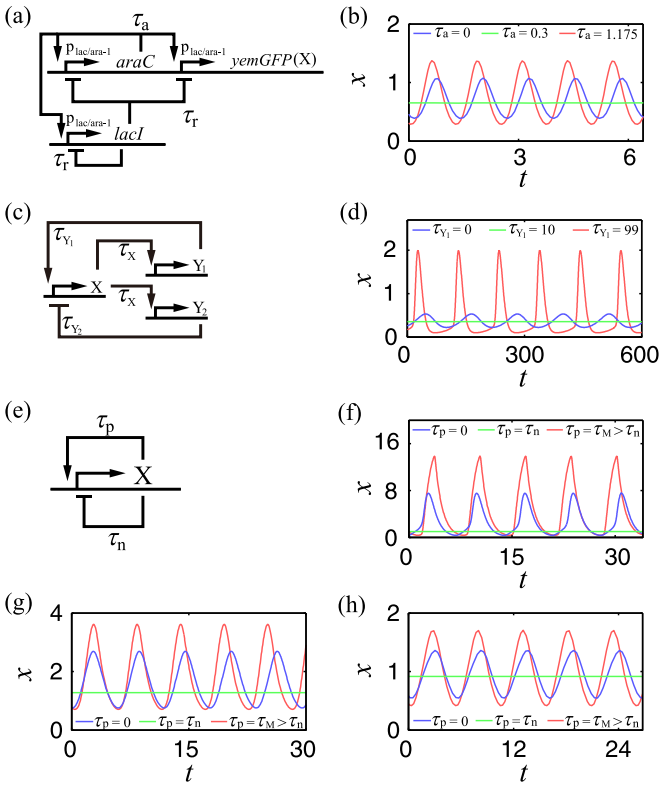

FIG. 1. Schematic of three models and the model dynamics. (a) The synthetic genetic circuit where the activator (*araC*), repressor (*lacI*), and reporter (*yemGFP*) are under the control of the same hybrid promoters $p_{lac/ara-1}$ (in two plasmids). τ_a and τ_r separately denote the time delays in production of araC and lacI proteins. (b) Time courses of the concentration of X for $\tau_r = 0.3$ and $\tau_a = 0$ (blue), 0.3 (green), or 1.175 (red). (c) A three-node model. The transcription factor X induces the production of Y_1 and Y_2. Y_1 (Y_2) activates (represses) the production of X. τ_X, τ_{Y_1}, and τ_{Y_2} separately denote the delays in production of X, Y_1, and Y_2. (d) Time courses of x for $\tau_{Y_2} = 1$ and $\tau_{Y_1} = 0$ (blue), 10 (green), or 99 (red). (e) A simplified model. X regulates the production of itself via positive and negative feedback. τ_p and τ_n denote the corresponding delays. [(f)–(h)] Time courses of x. Two feedback loops are coupled multiplicatively (f), additively (g), or competitively (h). $\tau_n = 1.8$ and τ_M denotes the minimal τ_p at which the largest amplitude is induced; $\tau_M = 6.4$ (f), 5.025 (g), or 4.6 (h).

kinetic equations are as follows [7]:

$$\frac{dY_a}{dt} = \alpha_a \frac{1 + k\frac{Y_a(t-\tau_a)}{C_1}}{\left[1 + \frac{Y_a(t-\tau_a)}{C_1}\right]\left[1 + \frac{Y_r(t-\tau_a)}{C_0}\right]^2} - \frac{\gamma_a Y_a}{R_0 + Y_a} - \beta Y_a, \quad (1)$$

$$\frac{dY_r}{dt} = \alpha_r \frac{1 + k\frac{Y_a(t-\tau_r)}{C_1}}{\left[1 + \frac{Y_a(t-\tau_r)}{C_1}\right]\left[1 + \frac{Y_r(t-\tau_r)}{C_0}\right]^2} - \frac{\gamma_r Y_r}{R_0 + Y_r} - \beta Y_r, \quad (2)$$

$$\frac{dx}{dt} = \alpha_x \frac{1 + k\frac{Y_a}{C_1}}{\left(1 + \frac{Y_a}{C_1}\right)\left(1 + \frac{Y_r}{C_0}\right)^2} - \frac{\gamma_x x}{R_0 + x} - \beta x, \quad (3)$$

where Y_a, Y_r, and x denote the concentrations of the activator, repressor, and reporter, respectively, while τ_a and τ_r separately denote the delays in the production of mature araC and lacI proteins. On the right-hand side of each equation, the first term denotes the production rate which is regulated by both the activator and the repressor, the second denotes the rate of enzymatic degradation by the protease, and the third denotes the degradation rate due to dilution. The functions for the production rates of proteins are taken based on a rapid equilibrium assumption that the multimerization and binding of proteins to the promoter are fast compared with gene expression and protein degradation [22,23]. α_a, α_r, and α_x correspond to the basal production rate; $k > 1$ characterizes the strength of positive feedback. C_1 and C_0 are the concentration thresholds for feedback regulation by the activator and repressor, respectively. The enzymatic degradation is described by the Michaelis-Menten kinetics with the maximal rate γ_i ($i = \{a,r,x\}$). The degradation due to dilution is considered a first-order reaction with a rate constant of β. Fixed parameters are set as follows: $\alpha_a = \alpha_r = \alpha_x = 4$, $k = 50$, $C_0 = C_1 = 0.3$, $\gamma_a = \gamma_x = 10$, $\gamma_r = 6.5$, $R_0 = 1$, $\beta = 0.1$, and $\tau_r = 0.3$; τ_a is a control parameter.

We simulate the circuit dynamics for three values of τ_a. Consistent with the previous results [7], the oscillation is suppressed with $\tau_a = \tau_r = 0.3$ [Fig. 1(b)]. Unexpectedly, the oscillation has a larger amplitude with $\tau_a = 1.175 > \tau_r$ than with $\tau_a = 0$, suggesting that the PFL with a long delay may facilitate large-amplitude oscillations.

Second, we probe a three-node model that represents a large class of coupled PFL and NFL [24]. The transcription factor X induces the production of Y_1 and Y_2, while Y_1 and Y_2 promote or repress, respectively, the induction of X [Fig. 1(c)]. The dynamics of the system are described by the following delayed differential equations (DDEs) [24]:

$$\frac{dx}{dt} = V_x \frac{\left[\frac{y_1(t-\tau_X)}{K_{y_1x}}\right]^n}{1 + \left[\frac{y_1(t-\tau_X)}{K_{y_1x}}\right]^n + \left[\frac{y_2(t-\tau_X)}{K_{y_2x}}\right]^n} - d_x x + b_x, \quad (4)$$

$$\frac{dy_1}{dt} = V_{y_1} \frac{\left[\frac{x(t-\tau_{Y_1})}{K_{xy_1}}\right]^n}{1 + \left[\frac{x(t-\tau_{Y_1})}{K_{xy_1}}\right]^n} - d_{y_1} y_1 + b_{y_1}, \quad (5)$$

$$\frac{dy_2}{dt} = V_{y_2} \frac{\left[\frac{x(t-\tau_{Y_2})}{K_{xy_2}}\right]^n}{1 + \left[\frac{x(t-\tau_{Y_2})}{K_{xy_2}}\right]^n} - d_{y_2} y_2 + b_{y_2}, \quad (6)$$

where x, y_1, and y_2 denote the concentrations of X, Y_1, and Y_2, respectively. On the right-hand side of each equation, the first term denotes the regulated production rate: The function for X represents the competitive regulation by Y_1 and Y_2, while those for Y_1 and Y_2 are standard Hill functions. V_{y_1} and V_{y_2} characterize the strength of positive and negative feedback, respectively. τ_X, τ_{Y_1}, and τ_{Y_2} separately denote the delays in production of X, Y_1, and Y_2. The first-order and constant terms describe the degradation rate and the basal production rate, respectively. Parameters are set as follows: $V_x = 20$, $K_{xy_1} = 1$, $K_{xy_2} = 1$, $K_{y_1x} = 1$, $K_{y_2x} = 1$, $b_x = 0.01$, $b_{y_1} = 0.1$, $b_{y_2} = 0.1$, $d_x = 0.2$, $d_{y_1} = 0.2$, $d_{y_2} = 0.02$, $V_{y_1} = 0.7$, $V_{y_2} = 2$, $n = 2$, and $\tau_X = \tau_{Y_2} = 1$. We simulate the model dynamics under three conditions with $\tau_{Y_1} = 0$, 10, or 99, and the phenomena similar to those in Fig. 1(b) are observed [Fig. 1(d)].

To test the generality of these results, we build a simplified model of the above synthetic circuit [Fig. 1(e)].

The concentration of X, x, reflects the promoter activity. A high promoter activity leads to high-level expression of the activator and repressor, thereby resulting in strong positive (negative) regulation of transcription. Thus, the feedback regulation can be simply described by a monotonic function of x with sufficient nonlinearity for the cooperativity and saturation, and intermediate steps in the PFL and NFL are replaced with a one-step process with a delay of τ_p and τ_n, respectively. With these simplifications, the synthetic circuit is modeled by a single-node system with two opposing delayed autoregulations, which can also be considered as a simplification of the above three-node model.

The deterministic dynamics of the simplified model are governed by the following DDE:

$$\frac{dX}{d\tilde{t}} = \tilde{\eta}_0 \tilde{F}_0(X_{\tilde{t}-\tilde{\tau}_p}, X_{\tilde{t}-\tilde{\tau}_n}) - \gamma X, \tag{7}$$

with $X = N/\Omega$, where N is the number of proteins, Ω is the volume of the cell, $X_{\tilde{t}-\tilde{\tau}_p} \equiv X(\tilde{t}-\tilde{\tau}_p)$, and $X_{\tilde{t}-\tilde{\tau}_n} \equiv X(\tilde{t}-\tilde{\tau}_n)$. On the right-hand side of Eq. (7), the first and second terms denote the production and degradation rates, respectively. γ is the degradation rate constant. The form of $\tilde{F}_0$ depends on the coupling manner of two feedback loops; here they are coupled multiplicatively, additively, or competitively [24,25]. For multiplicative coupling, $\tilde{F}_0(x,y) \equiv \tilde{f}_0(x)\tilde{g}_0(y)$, with $\tilde{f}_0(x) = \frac{k_{p0}+k_{p1}(x/K_p)^{m_p}}{1+(x/K_p)^{m_p}}$ and $\tilde{g}_0(y) = \frac{k_{n0}+k_{n1}(y/K_n)^{m_n}}{1+(y/K_n)^{m_n}}$. Parameters k_{p0}, k_{p1}, k_{n0}, and k_{n1} can take any value provided $k_{p1} > k_{p0} > 0$ and $0 \leqslant k_{n1} < k_{n0}$. m_p and m_n reflect the degree of nonlinearity; K_p and K_n characterize the concentration thresholds associated with feedback regulation. Notably, $\tilde{f}_0(x) \in [k_{p0}, k_{p1})$ and $\tilde{g}_0(y) \in (k_{n1}, k_{n0}]$ for $x, y \geqslant 0$, and they represent the effects of positive and negative feedback, respectively, due to $\frac{d}{dx}\tilde{f}_0(x) > 0$ and $\frac{d}{dy}\tilde{g}_0(y) < 0$. Given $\tilde{f}_0(0) = k_{p0}$ and $\tilde{g}_0(0) = k_{n0}$, $\tilde{\eta}_0 k_{p0} k_{n0}$ is the production rate without any regulation by the activator or repressor (i.e., $x = y = 0$). It is worth noting that similar functions to $\tilde{f}_0(x)$ and $\tilde{g}_0(y)$ were used to describe the nonlinear regulation with cooperativity and saturation [26,27]. Furthermore, $\tilde{f}_0(x)$ can be rewritten as $\tilde{f}_0(x) = k_{p0} + \frac{(k_{p1}-k_{p0})(x/K_p)^{m_p}}{1+(x/K_p)^{m_p}}$, equivalent to Eq. (3) in Ref. [28], and for $k_{n1} = 0$, $\tilde{g}_0(y) = \frac{k_{n0}}{1+(y/K_n)^{m_n}}$, similar to Eq. (1) in Ref. [29].

By setting $\alpha_p = k_{p1}/k_{p0}$, $\alpha_n = k_{n1}/k_{n0}$, and $\tilde{\eta} = \tilde{\eta}_0 k_{p0} k_{n0}$, we obtain a concise form of Eq. (7):

$$\frac{dX}{d\tilde{t}} = \tilde{\eta}\tilde{F}(X_{\tilde{t}-\tilde{\tau}_p}, X_{\tilde{t}-\tilde{\tau}_n}) - \gamma X, \tag{8}$$

where $\tilde{F}(x,y) \equiv \tilde{f}(x)\tilde{g}(y)$ with $\tilde{f}(x) = \frac{1+\alpha_p(x/K_p)^{m_p}}{1+(x/K_p)^{m_p}}$ ($\alpha_p > 1$) and $\tilde{g}(y) = \frac{1+\alpha_n(y/K_n)^{m_n}}{1+(y/K_n)^{m_n}}$ ($0 \leqslant \alpha_n < 1$). Still, $\tilde{f}$ and $\tilde{g}$ separately represent the effects of positive and negative feedback, thus describing the promotion and inhibition of the production. α_p and α_n denote the extent to which the production is modulated, and $\tilde{\eta}$ represents the maximal or minimal production rate of X for the NFL-only (with $\alpha_p = 1$) and PFL-only (with $\alpha_n = 1$) systems, respectively.

Furthermore, the dimensionless variables and parameters are defined as follows: $x \equiv X/K_n$, $K \equiv K_p/K_n$, $t \equiv \gamma\tilde{t}$, $\tau_p \equiv \gamma\tilde{\tau}_p$, $\tau_n \equiv \gamma\tilde{\tau}_n$, and $\eta \equiv \tilde{\eta}/(K_n\gamma)$, such that Eq. (8) is converted into a dimensionless form

$$\frac{dx}{dt} = \eta F(x_{t-\tau_p}, x_{t-\tau_n}) - x, \tag{9}$$

where $x_{t-\tau_p} \equiv x(t-\tau_p)$, $x_{t-\tau_n} \equiv x(t-\tau_n)$, and $F(u,v) \equiv f(u)g(v)$ with $f(u) = \frac{1+\alpha_p(u/K)^{m_p}}{1+(u/K)^{m_p}}$ and $g(v) = \frac{1+\alpha_n v^{m_n}}{1+v^{m_n}}$. The parameters are set as follows: $m_p = m_n = 4$, $\alpha_p = 10$, $\alpha_n = 0.02$, $K = 3$, $\eta = 1.767$, and $\tau_n = 1.8$.

Equation (9) also holds true for additive coupling except a different form of F:

$$F(x_{t-\tau_p}, x_{t-\tau_n}) = \beta f(x_{t-\tau_p}) + g(x_{t-\tau_n}), \tag{10}$$

with $\beta = 0.11$ and $\eta = 3$ (the other parameters remain the same). For competitive coupling,

$$F(x_{t-\tau_p}, x_{t-\tau_n}) = \frac{1+\alpha_p(x_{t-\tau_p}/K)^{m_p}}{1+(x_{t-\tau_p}/K)^{m_p} + \Gamma x_{t-\tau_n}^{m_n}}, \tag{11}$$

with $\alpha_p = 6$, $\Gamma = 1$, and $\eta = 1.5$ (the other parameters are unchanged). In each case, x remains constant with $\tau_p = \tau_n$; x oscillates at a larger amplitude with $\tau_p > \tau_n$ than with $\tau_p = 0$ [Figs. 1(f)–1(h)]. Together, these results consistently show that a PFL with a long delay may evoke large-amplitude oscillations.

III. INFLUENCE OF TIME DELAY ON THE STABILITY OF STEADY STATES

To quantitatively characterize the role for delayed PFL in modulating oscillation, we focus on the simplified model with multiplicative coupling. We first explore how time delays affect the stability of steady states. The steady-state equation is obtained by setting $dx/dt = 0$ and $x = x_{t-\tau_p} = x_{t-\tau_n} = x_s$ in Eq. (9):

$$\eta = \frac{x_s}{f(x_s)g(x_s)}, \tag{12}$$

where x_s is the steady-state level of x. For given η, the stability of the steady state is determined by the roots of the characteristic equation associated with Eq. (9):

$$\lambda + 1 - G_n e^{-\tau_n\lambda} - G_p e^{-\tau_p\lambda} = 0, \tag{13}$$

where $\lambda = \mu \pm i\omega$ ($\omega > 0$) is the characteristic root. $G_p \equiv G_p(x_s) = \frac{x_s}{f(x_s)}\frac{df(x)}{dx}|_{x_s} > 0$ and $G_n \equiv G_n(x_s) = \frac{x_s}{g(x_s)}\frac{dg(x)}{dx}|_{x_s} < 0$ are the logarithmic gains (called gain for short thereafter) of the PFL and NFL, respectively (see Ref. [27] for details). Notably, Eq. (13) has an infinite number of λ's. A steady state is stable if all λ's have a negative real part or unstable if some λ has a positive real part.

At $\lambda = 0$, the system may undergo saddle-node (SN) bifurcation, via which two/multiple steady states may arise. At the bifurcation point,

$$G_n + G_p = 1. \tag{14}$$

If no x_s obeys Eq. (14) for any η, the system never undergoes SN bifurcation. Obviously, a stronger condition for that is $G_n(x) + G_p(x) < 1$ over $x \in [0, +\infty)$. In this case, the

system always has only one steady state. For simplicity, we only discuss this case in the following.

At $\lambda = \pm i\omega$, the stability of this steady state may change via Hopf bifurcation. Substituting $\lambda = i\omega$ into Eq. (13) yields pairs of τ_p and τ_n for Hopf bifurcation:

$$\tau_\mathrm{n}^{j,k,l} = \frac{1}{\omega}\left[(-1)^j H_\mathrm{n}(\omega) + \tan^{-1}\frac{1}{\omega}\right] + \frac{(2k+j)\pi}{\omega}, \quad (15)$$

$$\tau_\mathrm{p}^{j,k,l} = \frac{1}{\omega}\left[(-1)^j H_\mathrm{p}(\omega) + \tan^{-1}\frac{1}{\omega}\right] + \frac{(2l+j)\pi}{\omega}, \quad (16)$$

with

$$H_\mathrm{n}(\omega) = \sin^{-1}\frac{G_\mathrm{p}^2 - G_\mathrm{n}^2 - 1 - \omega^2}{2G_\mathrm{n}\sqrt{1+\omega^2}}, \quad (17)$$

$$H_\mathrm{p}(\omega) = \sin^{-1}\frac{G_\mathrm{n}^2 - G_\mathrm{p}^2 - 1 - \omega^2}{2G_\mathrm{p}\sqrt{1+\omega^2}}, \quad (18)$$

$j = 0,1$; $k,l \in \mathbb{Z}_{\geqslant 0}$. For each set of $(j,\ k,\ l)$, the points $(\tau_\mathrm{n}^{j,k,l}, \tau_\mathrm{p}^{j,k,l})$ varying with ω constitute a Hopf bifurcation curve on the $(\tau_\mathrm{n}, \tau_\mathrm{p})$ plane. When τ_p or τ_n is varied to cross these curves, Hopf bifurcation occurs. Meanwhile, if all the other λ's keep their real parts negative, the stability of the steady state changes.

For comparison, we also analyze an NFL-only system with $\alpha_\mathrm{p} = 1$ [i.e., $f(x) = 1$]. η is adjusted such that the NFL-only system has the same steady state x_s as the coupled system. The critical value of τ_n, at which the steady state changes its stability, is

$$\tau_\mathrm{n,NFL} = \frac{\cos^{-1}\frac{1}{G_\mathrm{n}}}{\sqrt{G_\mathrm{n}^2 - 1}}, \quad (19)$$

where G_n equals that of the coupled system. When $G_\mathrm{n} < -1$ and $\tau_\mathrm{n} > \tau_\mathrm{n,NFL}$, the steady state becomes unstable.

We choose three specific sets of parameter values (see the caption of Fig. 2), which result in different values of $G_\mathrm{p} + G_\mathrm{n}$, to illustrate the influence of time delay on the stability of steady states. For $G_\mathrm{p} + G_\mathrm{n} < -1$, the Hopf bifurcation curves for different (j,k,l) are plotted on the $(\tau_\mathrm{n}, \tau_\mathrm{p})$ plane [Fig. 2(a), solid curves]. The leftmost cluster of curves constitutes the jagged boundary between the regions for stable and unstable steady states. Compared with the NFL-only system, parts of the boundary extend outward, whereas other parts hollow inward. Thus, the addition of a delayed PFL can either promote or inhibit the change of stability, which occurs repeatedly as τ_p rises due to the recurrence of Hopf bifurcation—each ω determines multiple pairs of $\tau_\mathrm{p}^{j,k,l}$ and $\tau_\mathrm{n}^{j,k,l}$, with the nearest pair separated by $2\pi/\omega$. Notably, the steady state can be unstable for any τ_p if τ_n is large enough.

Especially, the critical value of τ_n for $\tau_\mathrm{p} = 0$, $\tau_{\mathrm{n},0}$, is

$$\tau_{\mathrm{n},0} = \frac{\cos^{-1}\left(\frac{1-G_\mathrm{p}}{G_\mathrm{n}}\right)}{\sqrt{G_\mathrm{n}^2 - (1-G_\mathrm{p})^2}}, \quad (20)$$

and that for $\tau_\mathrm{p} = \tau_\mathrm{n}$, $\tau_\mathrm{n,eq}$, is

$$\tau_\mathrm{n,eq} = \frac{\cos^{-1}\left(\frac{1}{G_\mathrm{n}+G_\mathrm{p}}\right)}{\sqrt{(G_\mathrm{n}+G_\mathrm{p})^2 - 1}}. \quad (21)$$

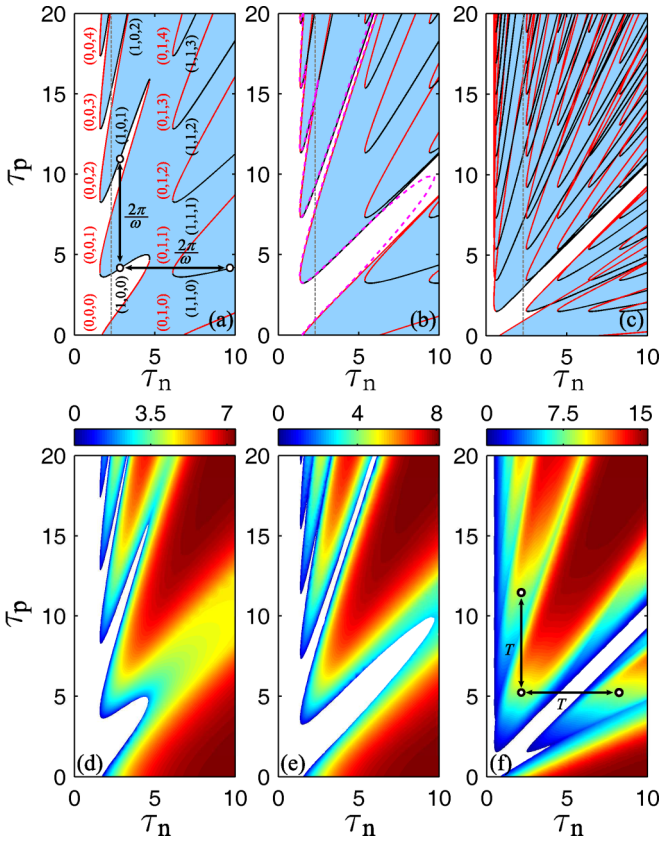

FIG. 2. Effects of time delays on Hopf bifurcation and oscillation amplitude. [(a)–(c)] Dependence of the stability of steady states on τ_p and τ_n. The red and black curves denote Hopf bifurcation curves determined by Eqs. (15) and (16), respectively. The curve marked by (j,k,l) is composed of the points $(\tau_n^{j,k,l}, \tau_p^{j,k,l})$ with $i = 0,1$ and $j,k = 0,1,2,\ldots$. The white and blue regions denote stable and unstable steady states, respectively. The gray dashed vertical line separates stable from unstable steady states for the NFL-only system. The circles and arrows denote the pointwise periodicity in delays for Hopf bifurcation. The magenta dashed curves in (b) denote the boundary of oscillatory behavior. [(d)–(f)] Dependence of oscillation amplitude on τ_n and τ_p. The amplitude is represented by the heat map. The circles and arrows refer to the delays for the same oscillation with period T. $m_\mathrm{p} = 4$, $m_\mathrm{n} = 2$, $\alpha_\mathrm{n} = 0.01$, $K = 2$ and $\tau_\mathrm{n} = 3$; $\alpha_\mathrm{p} = 1.35$ and $\eta = 5.738$ for $G_\mathrm{p} + G_\mathrm{n} < -1$ [(a) and (d)], $\alpha_\mathrm{p} = 1.57$ and $\eta = 5.376$ for $G_\mathrm{p} + G_\mathrm{n} = -1$ [(b) and (e)], $\alpha_\mathrm{p} = 10$ and $\eta = 1.573$ for $-1 < G_\mathrm{p} + G_\mathrm{n} < 1$ [(c) and (f)], or $\alpha_\mathrm{p} = 1$ and $\eta = 6.427$ for the NFL-only system.

Given the same x_s, $\tau_{\mathrm{n},0} < \tau_\mathrm{n,NFL} < \tau_\mathrm{n,eq}$. That is, compared with the NFL-only system, adding a nondelayed PFL reduces the critical value, facilitating the occurrence of Hopf bifurcation, whereas adding a PFL with the same delay increases the critical value, enhancing the stability.

As G_p is increased, $\tau_{\mathrm{n},0}$ drops but $\tau_\mathrm{n,eq}$ rises. For $-1 \leqslant G_\mathrm{p} + G_\mathrm{n} < 1$ (acquired by increasing the strength of the PFL, α_p, while keeping x_s and G_n unchanged by reducing η), there is no definition for $\tau_\mathrm{n,eq}$. Thus, the steady states at $\tau_\mathrm{p} = \tau_\mathrm{n}$ are always stable [Figs. 2(b) and 2(c)], which was also observed in Ref. [30]. Meanwhile, the regions of unstable steady states at $\tau_\mathrm{p} > \tau_\mathrm{n}$ tend to overlap and further enlarge,

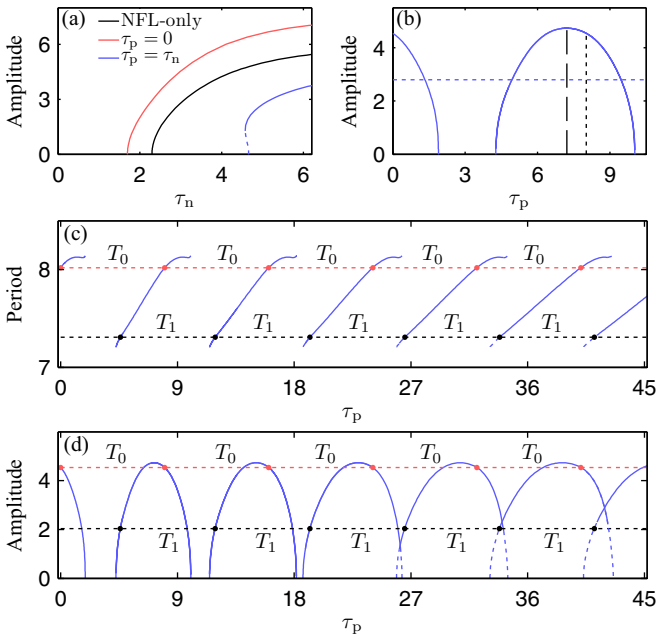

FIG. 3. Effects of time delays on the amplitude and period of oscillation. (a) Dependence of the amplitude on τ_n. Black, red, and blue curves correspond to the NFL-only system and the coupled systems with $\tau_p = 0$ and with $\tau_p = \tau_n$, respectively. (b) Dependence of the amplitude on τ_p at $\tau_n = 3$. The dashed horizontal line denotes the amplitude for the NFL-only system. The dashed and dotted vertical lines separately correspond to $\tau_p = 7.22$ and 8.02. The other parameter values are the same as in Fig. 2(a). [(c) and (d)] Dependence of the period (c) and amplitude (d) on τ_p in a wide range [the same parameters as in panel (b)]. The solid and dashed curves denote the stable and unstable limit cycles, respectively. Red and black dots denote the periodic solutions with the period of $T_0 = 8.02$ and $T_1 = 7.50$, respectively.

indicating that an lPFL with large G_p can always facilitate the induction of oscillation.

IV. EFFECT OF TIME DELAY ON THE OSCILLATORY DYNAMICS

Here, we probe how time delays affect the limit-cycle oscillation [Figs. 2(d)–2(f)]. Most oscillations occur within the region of unstable steady states, but for some τ_p and τ_n, oscillation may also coexist with a stable steady state (e.g., at $\tau_p = \tau_n = 10$). Remarkably, the amplitude A and period T change with τ_p and τ_n in a pointwise periodic manner, due to recurrence of periodic solutions [31]. If a limit cycle with period T occurs at τ_p and τ_n, it reappears at $\tau_n + kT$ and $\tau_p + lT$ with $k,l \in \mathbb{Z}$ (but its stability may change; see Appendix A for proof). Thus, both A and T are pointwise periodic functions of τ_n and τ_p, i.e., $A[\tau_n + kT(\tau_n,\tau_p), \tau_p + lT(\tau_n,\tau_p)] = A(\tau_n,\tau_p)$ and $T[\tau_n + kT(\tau_n,\tau_p), \tau_p + lT(\tau_n,\tau_p)] = T(\tau_n,\tau_p)$ with $k,l \in \mathbb{Z}$, in a range of delays.

Taking the system with $G_p + G_n < -1$ as an example, we show how the oscillation amplitude is affected by τ_n and τ_p. Compared with the NFL-only system, the coupled system with $\tau_p = 0$ has a larger amplitude, whereas that with $\tau_p = \tau_n$ has a smaller amplitude [Fig. 3(a)]. At $\tau_n = 3$, when τ_p rises from 0 to τ_n, the amplitude monotonically drops until the oscillation disappears [Fig. 3(b)]. For $\tau_p > \tau_n$, however, the oscillation can reappear, and the amplitude rises to its maximum at $\tau_p = 7.22$. The oscillation at $\tau_p = 0$ has the period of $T_0 = 8.02$; according to the recurrence of periodic solution, the oscillation has the same amplitude at $\tau_p = T_0$. In fact, periodic solutions with a period T_0 can appear at τ_p's with the nearest interval being T_0 [Figs. 3(c) and 3(d)], and the above change in oscillation amplitude repeats when τ_p continues rising from T_0 over some range [Fig. 3(d)]. For periodic solutions with a different period, e.g., $T_1 = 7.50$, they appear periodically with the nearest interval being T_1. Thus, when τ_p is sufficiently large, parts of solution branches overlap, and some oscillations may become unstable or coexist with one another to generate bi- or multirhythmic dynamics.

Notably, the maximal amplitude appears only when τ_p is large enough given $\tau_p \leqslant T_0$. To test whether this phenomenon is parameter specific, we sample 10 000 parameter sets for $K > 1$ and $K < 1$, respectively (see Table I in Appendix B for the ranges of parameter sampling), using the Latin hypercube sampling method (MATLAB built-in function *lhsdesign*). For each parameter set that satisfies $G_n < -1$ and $G_p + G_n < 1$, we calculate the minimal positive τ_p, τ_{pm}, at which the maximal amplitude is acquired. The histograms show that τ_{pm}/τ_n is always greater than 1 [Figs. 4(a) and 4(b)],

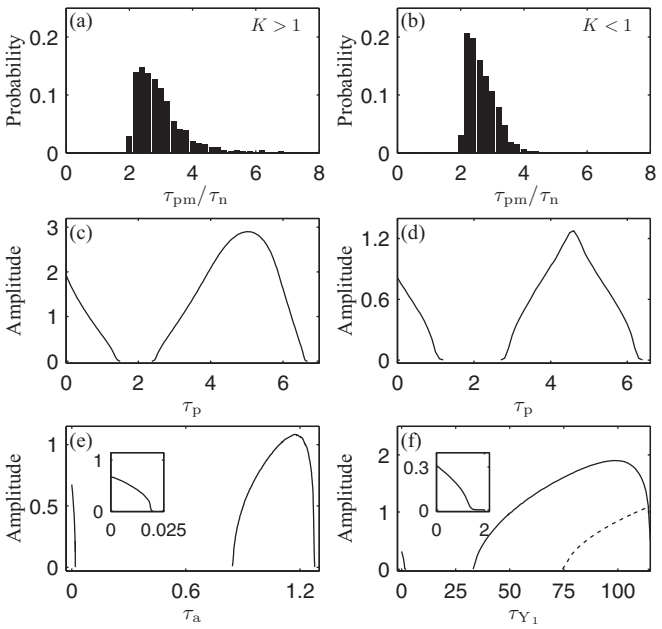

FIG. 4. Large-amplitude oscillations induced by the PFL with a long delay. [(a) and (b)] Statistic distributions for the minimal τ_p at which the maximal amplitude is acquired relative to τ_n. 1054 and 1030 sets of parameter values are sampled for $K > 1$ (a) and $K < 1$ (b), respectively. [(c)–(f)] Effects of τ_p on the oscillation amplitude in the simplified model with additive (c) or competitive (d) coupling, in the synthetic oscillator (e), and in the three-node model (f). The solid and dashed curves denote the stable and unstable limit cycles, respectively. The insets show the amplitude near $\tau_a = 0$ (e) or $\tau_{Y_1} = 0$ (f). See Sec. II for parameter values.

confirming that the above effect is robust against parameter perturbations.

Similar phenomena are observed in the simplified model with additive or competitive coupling [Figs. 4(c) and 4(d)], as well as in the synthetic oscillator model [Fig. 4(e)] and the three-node model [Fig. 4(f)], indicating that such an impact of τ_p on oscillation amplitude is independent of the coupling manner and details in the model. Collectively, the PFL with a properly long delay can facilitate large-amplitude oscillations.

V. MODULATION OF OSCILLATION BY THE DELAYED PFL

To unravel the essential mechanism for the regulation of oscillation amplitude by the delayed PFL, we consider a limiting case of $m_p, m_n \to +\infty$, in which sigmoid functions f and g are replaced with step functions:

$$f(u) = \begin{cases} 1, & 0 \leqslant u < K, \\ \alpha_p, & u \geqslant K, \end{cases} \tag{22}$$

and

$$g(v) = \begin{cases} 1, & 0 \leqslant v < 1, \\ \alpha_n, & v \geqslant 1. \end{cases} \tag{23}$$

That is, each loop has only two states: activated ($f = \alpha_p$ or $g = \alpha_n$) and deactivated ($f = 1$ or $g = 1$).

To simplify analytical calculation, we assume that α_p is relatively small such that $\alpha_p\alpha_n \approx \alpha_n$. Consequently, F is denoted as follows:

$$F(u,v) = \begin{cases} \alpha_n, & v \geqslant 1, \\ 1, & 0 \leqslant u < K, 0 \leqslant v < 1, \\ \alpha_p, & u \geqslant K, 0 \leqslant v < 1. \end{cases} \tag{24}$$

Thus, the activated PFL has no contribution to F if the NFL is activated simultaneously. Without loss of generality, we only discuss the case of $1 < K < \eta < \frac{1}{\alpha_n}$ and $\tau_n > \ln\frac{1-\eta}{K-\eta}$, where the system with $\tau_p = 0$ can undergo oscillations, during which the PFL can be activated with a higher threshold than the NFL (see Appendix C).

We calculate the oscillation trajectories of $x(t)$ starting from its minimum $x_{\min}$ at $t = 0$. The calculation shows

$$x_{\min} = e^{-\tau_n}(1 - \eta\alpha_n) + \eta\alpha_n, \tag{25}$$

which remains constant for any τ_p. In contrast, the maximum of $x(t)$ depends on τ_p. For $\tau_p \in [0, \tau_n + \epsilon_1)$ with $\epsilon_1 = \ln\frac{K-\eta}{1-\eta} < 0$,

$$x_{\max,1} = [e^{-\tau_n}(K - \eta) + e^{-(\tau_n-\tau_p)}\eta(1 - \alpha_p)]\frac{1-\eta}{K-\eta} + \eta\alpha_p. \tag{26}$$

For $\tau_p \in [\tau_n + \epsilon_1, \tau_n + \epsilon_2]$ with $\epsilon_2 = \ln\frac{K-\eta\alpha_n}{1-\eta\alpha_n} > 0$,

$$x_{\max,2} = e^{-\tau_n}(1 - \eta) + \eta. \tag{27}$$

Of note, $\frac{dx_{\max,1}}{d\tau_p} < 0$ and $x_{\max,1} \geqslant x_{\max,2}$ (see Appendix C 2). Therefore, the amplitude, $x_{\max} - x_{\min}$, monotonically drops with increasing τ_p over $[0, \tau_n + \epsilon_1)$ and remains unchanged over $[\tau_n + \epsilon_1, \tau_n + \epsilon_2]$.

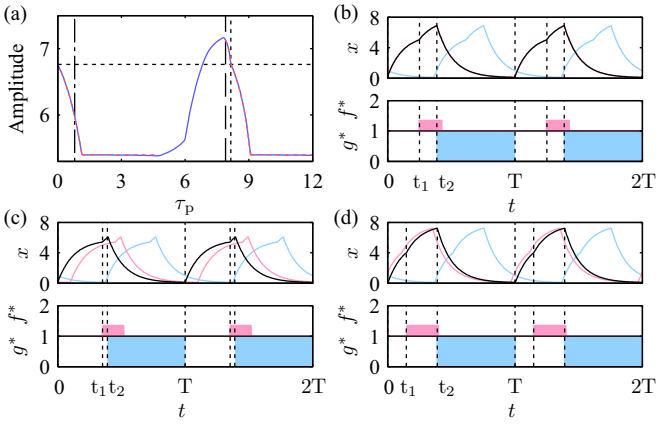

FIG. 5. Dynamics of the simplified model with $m_p, m_n \to +\infty$. (a) Dependence of the amplitude on τ_p. The blue and red curves denote the analytical and numerical results, respectively. The dashed horizontal line marks the amplitude for $\tau_p = 0$. The dot-dashed, dashed, and dotted vertical lines correspond to $\tau_p = 0.8$, 7.9, and 8.152, respectively. [(b)–(d)] Upper panels: The black, magenta, and blue curves denote $x(t)$, $x_{t-\tau_p}$, and $x_{t-\tau_n}$, respectively. Lower panels: $f^* \equiv f(x_{t-\tau_p})$ and $g^* \equiv g(x_{t-\tau_n})$. Parameter values are as follows: $K = 5$; (b) $\tau_p = 0$ and $T = T_0 = 8.152$; (c) $\tau_p = 0.8$ and $T = 8.034$; (d) $\tau_p = 7.9$ and $T = 8.203$. The other parameter values are the same as in Fig. 2(a).

We can extend the above calculation to $\tau_p = \tau_p' < 0$ (more exactly, τ_p' is marginally smaller than 0) and infer the amplitude for $\tau_p = \tau_p' + kT(\tau_n, \tau_p')$ ($k \in \mathbb{Z}^+$). For a very small $|\tau_p'|$ (see Appendix C 3),

$$x_{\max,\tau_p'<0} = \frac{e^{-\tau_p'-\tau_n}(K - \eta\alpha_p)(1-\eta)}{e^{-\tau_p'}(K - \eta\alpha_p) + \eta(\alpha_p - 1)} + \eta\alpha_p. \tag{28}$$

Given $x_{\max,\tau_p'<0} > x_{\max,1}$, there must be a $\tau_p = \tau_p' + T(\tau_n, \tau_p') > 0$ that allows for the oscillation amplitude greater than $x_{\max,\tau_p=0}$.

For a specific set of parameters satisfying the above conditions, the amplitude calculated numerically is well consistent with the analytical result [Fig. 5(a)]. Both results show low-amplitude oscillations at $\tau_p \approx \tau_n$ and larger-amplitude oscillations when τ_p approaches T_0.

To interpret the dependence of the amplitude on τ_p, $g^* \equiv g(x_{t-\tau_n})$ and $f^* \equiv f(x_{t-\tau_p})$ are plotted to show how the NFL and PFL are activated along with $x_{t-\tau_n}$ and $x_{t-\tau_p}$. For $\tau_p = 0$, $x(t)$ and $x_{t-\tau_p}$ coincide with each other [Fig. 5(b)]. In the ascending phase of $x(t)$ from $t = 0$, x first rises with the production rate η, until the PFL is activated at $t = t_1$ [$x(t_1) = K$], with

$$t_1 = \tau_p + \ln\frac{e^{-\tau_n}(1 - \eta\alpha_n) - \eta(1 - \alpha_n)}{K - \eta}. \tag{29}$$

Then, the rise of x is accelerated by the PFL with the maximal production rate $\eta\alpha_p$. The acceleration stops on the activation of the NFL at $t = t_2$ [$x_{t_2-\tau_n} = 1$], with

$$t_2 = \tau_n + \ln\frac{e^{-\tau_n}(1 - \eta\alpha_n) - \eta(1 - \alpha_n)}{1 - \eta}. \tag{30}$$

Afterwards, the production rate equals the minimum $\eta\alpha_n$, and the descending phase of x begins.

If τ_p is slightly larger than 0, then Eqs. (29) and (30) still hold true (see Appendix C 2), indicating that t_2 keeps unchanged but t_1 rises with τ_p. Thus, the rise of $x(t)$ is accelerated by the PFL over a shorter time period (i.e., $t_2 - t_1$), and the oscillation amplitude drops with increasing τ_p [Fig. 5(c)]. If τ_p' is marginally smaller than 0, then Eq. (30) still holds true, but t_1 becomes

$$t_1 = \ln \frac{e^{-\tau_n}(1-\eta\alpha_n) - \eta(1-\alpha_n)}{e^{-\tau_p'}(K-\eta\alpha_p) + \eta(\alpha_p - 1)}, \tag{31}$$

rising with increasing τ_p' (see Appendix C 3). Consequently, $x(t)$ is driven to greater values over an extended time period by the PFL, leading to a larger amplitude. According to the recurrence of periodic solutions, the PFL with $\tau_p = \tau_p' + kT(\tau_n, \tau_p') > 0$ ($k \in \mathbb{Z}^+$) also induces a larger-amplitude oscillation; in this case, the delayed PFL accelerates the rise of $x(t + kT)$ over a longer time period [e.g., $k = 1$; Fig. 5(d)]. Taken together, we explain why the PFL with a properly long delay has advantages over the nPFL and sPFL in terms of activation dynamics of feedback loops.

VI. ROBUST OSCILLATION INDUCED BY A STRONG lPFL

As α_p rises, the modulation of oscillation by the delayed PFL can be much more complicated. For example, limit cycles can coexist via the fold bifurcation of limit cycles when $\tau_p > \tau_n = 1.8$ [Fig. 6(a); black dots]; one stable and one unstable limit cycle appear together at $\tau_p = 6.245$ or collide to disappear at $\tau_p = 7.019$. Notably, the delayed PFL can facilitate larger-amplitude oscillations than the nondelayed PFL in a wide range of τ_p ($\in [3.81, 7.019]$). Moreover, the amplitudes of these oscillations are much greater compared with the case of small α_p.

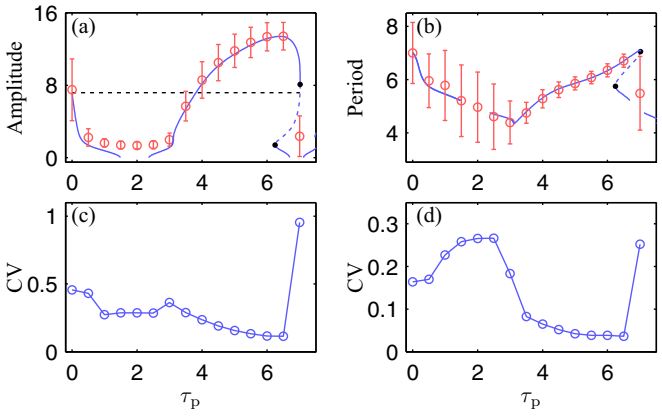

FIG. 6. Role for the strong PFL in modulating oscillatory dynamics. [(a) and (c)] Dependence of the oscillation amplitude and its CV on τ_p. The dashed horizontal line marks the amplitude for $\tau_p = 0$. [(b) and (d)] The oscillation period and its CV versus τ_p. The blue solid and dashed curves in [(a) and (b)] denote the stable and unstable limit cycles, respectively, in the deterministic case. Black dots at $\tau_p = 6.245$ and 7.019 denote the fold bifurcation of limit cycle. The circles and bars denote the mean and the standard deviation, respectively, in the stochastic case. Each stochastic simulation is run over [0,20000]. The amplitude is rescaled by $K_n\Omega = 10$. $m_p = 4$, $m_n = 4$, $\alpha_p = 10$, $\alpha_n = 0.02$, $K = 3$, $\eta = 1.767$, and $\tau_n = 1.8$.

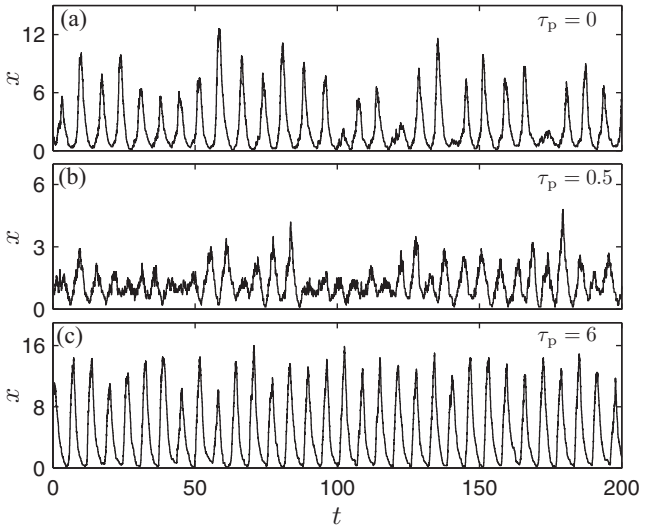

FIG. 7. Stochastic simulation of the simplified model. Sample trajectories of x for $\tau_p = 0$ (a), 0.5 (b), or 6 (c). The amplitude is rescaled by $K_n\Omega = 10$. The other parameters are the same as in Fig. 6.

It has been demonstrated that large amplitudes may be associated with relatively small fluctuations in oscillation [7]; thus, the PFL with a properly long delay may be advantageous over the nPFL and sPFL in ensuring the robustness of oscillation. To validate this inference, we need to perform stochastic simulations. There are two reactions in the simplified model: One is a delayed production of proteins, and the other is a nondelayed degradation of proteins. Whereas several stochastic simulation algorithms for delayed reactions were proposed [32–36], an algorithm for simulating a single reaction with two time delays is lacking. We extend the original Gillespie method to simulate this type of non-Markovian reaction based on the standard Monte Carlo method (see Appendix D).

We perform long-term stochastic simulations for different τ_p in the case of strong lPFL and then calculate the mean, standard deviation, and coefficient of variation (CV) of the peak-to-trough amplitude and interpeak period. The minimum of CV appears at the same τ_p as the maximal amplitude does [Figs. 6(c) and 6(d)]; that is, the lPFL can facilitate the oscillations with much smaller fluctuations in both the amplitude and period than the nPFL or sPFL [Fig. 7]. Thus, the PFL with a properly long delay can enhance the robustness of oscillation and accuracy of timing.

VII. DISCUSSION

We systematically explore how time delays in feedback regulation affect the dynamics of the systems of interlinked PFL and NFL. Compared with the NFL-only system, the delayed PFL can either promote or inhibit the occurrence

of oscillation, depending on its delay relative to that of the NFL. The PFL with a properly long delay can facilitate larger-amplitude oscillations than the nondelayed PFL, in contrast to the previous view that the shorter the delay, the more effectively the PFL can promote amplitude increment. We unravel two mechanisms for the realization of large-amplitude oscillations: the lPFL with weak strength can accelerate the accumulation of circuit components in an extended ascending phase because of its advanced activation, or the fold bifurcation of limit cycle can be induced in the presence of the lPFL with strong strength, leading to stable limit cycles with large amplitude.

To make full use of the PFL in promoting reliable oscillation, the required conditions proposed previously include faster dynamics of the activator than the repressor if no explicit feedback delay exists [37,38], a long delay in the NFL [39], or a short delay in the PFL [7], such that the activator can reach a higher level and have a stronger contributory role before the repressive effect from the repressor becomes too great [40]. Here, the PFL with a properly long delay can also contribute to robust oscillation via the similar mechanism, even playing a more marked role in driving large-amplitude oscillations.

Our results suggest an informative method for synthesizing robust genetic oscillators, i.e., the PFL should have a properly longer delay than the NFL. Such a design principle can be tested in the synthetic circuits as in Ref. [5], which include interlinked PFL and NFL with independently controllable effective time delays. Another plausible system is a recently developed synthetic genetic circuit involving efflux pumps [41]. It was shown that efflux pumps can introduce implicit negative feedback to the inducer (e.g., antibiotics) that regulates the circuit, thereby markedly altering the dose-response relationship. It seems possible to change the circuit design by adding PFLs as well as interlinking PFL and NFL with various time delays, so our conclusions can be justified in this system.

The current work can account for the presence of long delays in positive feedback in circadian clocks. Indeed, PER (PER1–PER3) and CRY (CRY1 and CRY2) in mammals form a dimer to repress the expression of their own genes, constituting an NFL; CRY1 can inhibit the expression of *Rev*-erbα, and Rev-erbα in turn represses the transcription of *cry1*, enclosing a PFL. That is, the PFL involves one extra process of *Rev*-erbα expression [21]. An earlier study on the circadian clock in *Neurospora crassa* also introduced a PFL with a long delay into the model [42]. WCC regulates the transcription of *frq*, and FRQ in turn phosphorylates WCC to inhibit its transcriptional activity, constituting an NFL; meanwhile, FRQ can promote the production of WC-1 and WC-2, which assemble into WCC, thereby constituting a PFL. Of note, the PFL involves one more translation process than the NFL [15], and thus the PFL has a longer effective delay than the NFL. Based on our results, such topologies can accommodate robust large-amplitude oscillations and precise timing.

Besides coupled dual-loop systems, interlinked multiple loops are also engaged in biological oscillating systems. For example, the mammalian circadian clock includes at least two more loops—the BMAL1-Rora PFL and BMAL1-Rev-Erbα NFL [43,44], in addition to the NFL involving PER/CRY self-repression and the PFL including REV-erbα. It is worth exploring how these multiple delayed loops coordinate robust oscillations. Moreover, several studies probed the synchronization of coupled oscillators, each consisting of delayed PFL and NFL [45–47]. The influence of PFLs with a long delay in each oscillator on the global dynamics is an open issue.

ACKNOWLEDGMENTS

This work was supported by National Basic Research Program of China (973 program) (Grant No. 2013CB834104) and the National Natural Science Foundation of China (Grants No. 11175084, No. 31361163003, and No. 81421091).

APPENDIX A: PROOF OF THE PERIODICITY OF TIME DELAY FOR THE SAME OSCILLATION

Lemma 1. If a delayed differential equation $\frac{dx}{dt} = F[x(t-\tau)]$ has a periodic solution $\hat{x}(t)$ with period T, then $\hat{x}(t)$ is also the solution to $\frac{dx}{dt} = F\{x[t-(\tau+nT)]\}$, with $n = 0,1,2,\ldots$.

Proof. Given $\hat{x}(t)$ is a periodic solution with period T, $\hat{x}(t-nT)$ is also a solution. Therefore, $\hat{x}(t-\tau) = \hat{x}(t-\tau-nT) = \hat{x}[t-(\tau+nT)]$. So, we have $\frac{d\hat{x}}{dt} = F[\hat{x}(t-\tau)] = F\{\hat{x}[t-(\tau+nT)]\}$, which shows that $\hat{x}(t)$ is also a solution to the equation with delay $\tau+nT$.

Lemma 2. If a delayed differential equation $\frac{dx}{dt} = F[x(t-\tau_1),x(t-\tau_2),\ldots]$ has a periodic solution $\hat{x}(t)$ with period T, then $\hat{x}(t)$ is also a solution to $\frac{dx}{dt} = F\{x[t-(\tau_1+n_1T)],x[t-(\tau_2+n_2T)],\ldots\}$, with $n_i = 1,2,\ldots$ $(i = 1,2,\ldots)$.

Proof. Given $\hat{x}(t)$ is a periodic solution with period T, $\hat{x}(t-n_iT)$ is also a solution. Therefore, $\hat{x}(t-\tau_i) = \hat{x}(t-\tau_i-n_iT) = \hat{x}[t-(\tau_i+n_iT)]$. So, we have $\frac{dx}{dt} = F\{x[t-(\tau_1+n_1T)],x[t-(\tau_2+n_2T)],\ldots\}$.

APPENDIX B: METHOD FOR PARAMETER SAMPLING

Ten thousand parameter sets are sampled uniformly on a logarithmic scale in a seven-dimensional parameter space using the Latin hypercube sampling method for $K > 1$ and $K < 1$, respectively. For each set of parameters satisfying $G_n < -1$ and $\max_{x\in[0,+\infty)}\{G_n(x)+G_p(x)\} < 1$ (1054 sets for $K > 1$ and 1030 sets for $K < 1$ in total), we calculate the critical value of τ_n for $\tau_p = 0$, $\tau_{n,0}$, as follows:

$$\tau_{n,0} = \frac{\cos^{-1}\left(\frac{1-G_p}{G_n}\right)}{\sqrt{G_n^2-(1-G_p)^2}}. \tag{B1}$$

Then, τ_n is set to $\delta\tau_{n,0}$; in this way, this set of parameters can lead to oscillation at $\tau_p = 0$.

TABLE I. Sampling ranges of the parameters.

	η	m_p	m_n	α_p	α_n	K	δ
$K > 1$	0.1–10	1–10	1–10	1–100	0.01–1	1–10	1–4
$K < 1$	0.1–10	1–10	1–10	1–100	0.01–1	0.1–1	1–4

APPENDIX C: THE CASE OF $m_p, m_n \to +\infty$

The deterministic dynamics of the simplified one-node model are governed by the following equation:

$$\frac{dx}{dt} = \eta F(x_{t-\tau_p}, x_{t-\tau_n}) - x, \tag{C1}$$

where $x_{t-\tau_p} \equiv x(t-\tau_p)$, $x_{t-\tau_n} \equiv x(t-\tau_n)$, and $F(u,v) \equiv f(u)g(v)$ with $f(u) = \frac{1+\alpha_p(u/K)^{m_p}}{1+(u/K)^{m_p}}$ and $g(v) = \frac{1+\alpha_n v^{m_n}}{1+v^{m_n}}$. Here, we discuss the scenario where $m_p, m_n \to +\infty$ such that sigmoid functions f and g can be replaced with step functions:

$$f(u) = \begin{cases} 1, & 0 \leqslant u < K, \\ \alpha_p, & u \geqslant K, \end{cases} \tag{C2}$$

and

$$g(v) = \begin{cases} 1, & 0 \leqslant v < 1, \\ \alpha_n, & v \geqslant 1. \end{cases} \tag{C3}$$

For simplicity, we only discuss the case of a weak PFL, i.e., $\alpha_p\alpha_n \approx \alpha_n$. Thus, F is simplified into

$$F(u,v) = \begin{cases} \alpha_n, & v \geqslant 1, \\ 1, & 0 \leqslant u < K, 0 \leqslant v < 1, \\ \alpha_p, & u \geqslant K, 0 \leqslant v < 1. \end{cases} \tag{C4}$$

The PFL can exert an effect, i.e., $F = \alpha_p$, only if $0 \leqslant v < 1$; otherwise, F always equals α_n. F reaches its maximum α_p if only the PFL is activated, while F equals its minimum α_n as long as the NFL is activated. Without loss of generality, here we only discuss the case of $K > 1$, i.e., the PFL has a higher activation threshold than the NFL.

Note that the activation threshold of the NFL is 1. If $\eta < 1$, $x(t) = \eta$ is a solution to Eq. (C1), and both feedback loops cannot be activated; if $\eta\alpha_n > 1$, then $x(t) = \eta\alpha_n$ is also a solution, and the NFL is always activated. If $\tau_n = 0$, then $x(t) = 1$ is a solution. In these cases, there is no oscillation. Only if $\eta\alpha_n < 1 < \eta$, i.e., $1 < \eta < \frac{1}{\alpha_n}$, and $\tau_n > 0$, can the system oscillate. On the other hand, if $K > \eta$, then x can only approach η in the ascending phase, and x cannot exceed K. To activate the PFL, one necessary condition is $K < \eta$. Together, here we assume $1 < K < \eta < \frac{1}{\alpha_n}$ and $\tau_n > 0$.

1. $\tau_p = 0$

First, we analyze the scenario of $\tau_p = 0$, i.e., $x(t) = x_{t-\tau_p}$. Suppose that the ascending phase of $x(t)$ starts from $t = 0$, at which the NFL switches from the activated state to the deactivated state, i.e., $x_{t-\tau_n} = 1$. $x(t)$ then rises, whereas $x_{t-\tau_n}$ continues falling. Since the minimum of $x(t)$, $x_{\min}$, is the same as the minimum of $x_{t-\tau_n}$, $x_{\min}$ must be less than 1. Due to $K > 1$, the PFL is also deactivated at this stage. $x(t)$ rises to η asymptotically with $F = \eta$. When $x(t)$ rises to K ($K < \eta$) at $t = t_1$ before $x_{t-\tau_n}$ equals 1, the PFL is activated and then accelerates the rise of $x(t)$ to $\eta\alpha_p$ asymptotically with $F = \eta\alpha_p$. When $x_{t-\tau_n}$ reaches 1 at $t = t_2$, the NFL is activated. The descending phase of $x(t)$ then starts, and $x(t)$ falls to $\eta\alpha_n$ asymptotically with $F = \eta\alpha_n$. When $x_{t-\tau_n} = 1$ again at $t = T$, the next round of ascending phase of $x(t)$ begins.

Over one period of oscillation, $x(t)$ goes through three stages. In the first stage, i.e., from $t = 0$ to $t = t_1$, $x(t)$ rises with t as follows:

$$x(t) = C_1 e^{-t} + \eta. \tag{C5}$$

In the second stage, i.e., from $t = t_1$ to $t = t_2$, the rise of $x(t)$ is accelerated, and $x(t)$ is

$$x(t) = C_2 e^{-(t-t_1)} + \eta\alpha_p. \tag{C6}$$

In the third stage, i.e., from $t = t_2$ to $t = T$, $x(t)$ decreases with t:

$$x(t) = C_3 e^{-(t-t_2)} + \eta\alpha_n. \tag{C7}$$

Six parameters, C_1, C_2, C_3, t_1, t_2, and T, are determined by the following six conditions:

$$\begin{aligned} C_1 e^{-t_1} + \eta &= C_2 + \eta\alpha_p, \\ C_2 e^{-(t_2-t_1)} + \eta\alpha_p &= C_3 + \eta\alpha_n, \\ C_3 e^{-(T-t_2)} + \eta\alpha_n &= C_1 + \eta, \\ C_1 e^{-(t_2-\tau_n)} + \eta &= 1, \\ C_2 + \eta\alpha_p &= K, \\ C_3 e^{-(T-t_2-\tau_n)} + \eta\alpha_n &= 1. \end{aligned} \tag{C8}$$

Six parameters can be solved:

$$\begin{aligned} C_1 &= e^{-\tau_n}(1-\eta\alpha_n) - \eta(1-\alpha_n) < 0, \\ t_1 &= \ln\frac{C_1}{K-\eta} > 0, \\ t_2 &= \tau_n + \ln\frac{C_1}{1-\eta} > 0, \\ C_2 &= K - \eta\alpha_p < 0, \\ C_3 &= C_2 e^{-(t_2-t_1)} + \eta(\alpha_p - \alpha_n) > 0, \\ T &= t_2 + \ln\frac{C_3}{C_1 + \eta(1-\alpha_n)} > 0. \end{aligned} \tag{C9}$$

If the NFL is activated in advance such that $x(t)$ does not rises to K yet, the descending phase of $x(t)$ begins earlier, and the PFL cannot be activated. This happens with $t_1 = t_2$, which requires $\tau_n = \ln\frac{1-\eta}{K-\eta}$. Thus, for the PFL to be activated earlier than the NFL,

$$\tau_n > \ln\frac{1-\eta}{K-\eta}. \tag{C10}$$

Then, we can calculate $x_{\min}$

$$x_{\min} = C_1 + \eta = e^{-\tau_n}(1-\eta\alpha_n) + \eta\alpha_n, \tag{C11}$$

and the maximum of $x(t)$ for $\tau_p = 0$,

$$\begin{aligned} x_{\max,0} &= C_3 + \eta\alpha_n \\ &= e^{-\tau_n}\frac{(K-\eta\alpha_p)(1-\eta)}{K-\eta} + \eta\alpha_p. \end{aligned} \tag{C12}$$

2. $\tau_p > 0$

For $\tau_n > \ln\frac{1-\eta}{K-\eta}$, the PFL with $\tau_p = 0$ can be activated before the NFL is activated at $t = t_1$. If $\tau_p > 0$, however, the activation of the PFL is delayed and may be later than the activation of the NFL. If $t_1 = t_2$, two feedback loops

are activated simultaneously, and the PFL has no effects. In this case, $\tau_p = \tau_n + \ln\frac{K-\eta}{1-\eta} < \tau_n$. Denote $\ln\frac{K-\eta}{1-\eta}$ by ϵ_1. If $0 \leqslant \tau_p < \tau_n + \epsilon_1$, then $x(t)$ goes through three states in one period of oscillation as in the case of $\tau_p = 0$ [see Eqs. (C5)–(C7)]. The conditions for the undetermined parameters are

$$\begin{aligned} C_1 e^{-t_1} + \eta &= C_2 + \eta\alpha_p, \\ C_2 e^{-(t_2-t_1)} + \eta\alpha_p &= C_3 + \eta\alpha_n, \\ C_3 e^{-(T-t_2)} + \eta\alpha_n &= C_1 + \eta, \\ C_1 e^{-(t_2-\tau_n)} + \eta &= 1, \\ C_1 e^{-(t_1-\tau_p)} + \eta &= K, \\ C_3 e^{-(T-t_2-\tau_n)} + \eta\alpha_n &= 1. \end{aligned} \tag{C13}$$

Six parameters can be solved subsequently:

$$\begin{aligned} C_1 &= e^{-\tau_n}(1-\eta\alpha_n) - \eta(1-\alpha_n) < 0, \\ t_1 &= \tau_p + \ln\frac{C_1}{K-\eta}, \\ t_2 &= \tau_n + \ln\frac{C_1}{1-\eta}, \\ C_2 &= e^{-\tau_p}(K-\eta) + \eta(1-\alpha_p) < 0, \\ C_3 &= C_2 e^{-(t_2-t_1)} + \eta(\alpha_p - \alpha_n) > 0, \\ T &= t_2 + \ln\frac{C_3}{C_1 + \eta(1-\alpha_n)}. \end{aligned} \tag{C14}$$

Then, we have

$$x_{\min} = C_1 + \eta = e^{-\tau_n}(1-\eta\alpha_n) + \eta\alpha_n, \tag{C15}$$

$$\begin{aligned} x_{\max,1} &= C_3 + \eta\alpha_n \\ &= [e^{-\tau_n}(K-\eta) + e^{-(\tau_n-\tau_p)}\eta(1-\alpha_p)]\frac{1-\eta}{K-\eta} + \eta\alpha_p. \end{aligned} \tag{C16}$$

$x_{\min}$ is independent of τ_p, while $x_{\max,1}$ depends on τ_p. Since the derivative of $x_{\max,1}$ with respect to τ_p,

$$\frac{dx_{\max,1}}{d\tau_p} = e^{-(\tau_n-\tau_p)}\frac{\eta(1-\alpha_p)(1-\eta)}{K-\eta} < 0, \tag{C17}$$

$x_{\max,1}$ decreases with τ_p given $0 \leqslant \tau_p < \tau_n + \epsilon_1$.

For $\tau_p \geqslant \tau_n + \epsilon_1$, the PFL may lose its effect due to the activation of the NFL. Thus, the rise of $x(t)$ is no longer accelerated, and $x(t)$ just goes through two stages in one period of oscillation. In the first stage, i.e., from $t = 0$ to $t = t_1$, $x(t)$ rises with $F = \eta$,

$$x(t) = C_1 e^{-t} + \eta. \tag{C18}$$

In the second stage, i.e., from $t = t_1$ to $t = T$, $x(t)$ decreases with $F = \eta\alpha_n$,

$$x(t) = C_2 e^{-(t-t_1)} + \eta\alpha_n. \tag{C19}$$

The conditions for the undetermined parameters are

$$\begin{aligned} C_1 e^{-t_1} + \eta &= C_2 + \eta\alpha_n, \\ C_2 e^{-(T-t_1)} + \eta\alpha_n &= C_1 + \eta, \\ C_1 e^{-(t_1-\tau_n)} + \eta &= 1, \\ C_2 e^{-(T-t_1-\tau_n)} + \eta\alpha_n &= 1. \end{aligned} \tag{C20}$$

Four parameters, C_1, C_2, t_1, and T, are solved subsequently:

$$\begin{aligned} C_1 &= e^{-\tau_n}(1-\eta\alpha_n) - \eta(1-\alpha_n) < 0, \\ C_2 &= e^{-\tau_n}(1-\eta) - \eta(\alpha_n - 1) > 0, \\ t_1 &= \tau_n + \ln\frac{C_1}{1-\eta}, \\ T &= t_1 + \ln\frac{C_2}{C1 + \eta(1-\alpha_n)}. \end{aligned} \tag{C21}$$

Then we have

$$x_{\min} = C_1 + \eta = e^{-\tau_n}(1-\eta\alpha_n) + \eta\alpha_n, \tag{C22}$$

$$x_{\max,2} = C_2 + \eta\alpha_n = e^{-\tau_n}(1-\eta) + \eta. \tag{C23}$$

If τ_p is large enough, then the PFL can be deactivated later than the NFL. Thus, the PFL can still be activated when the NFL is deactivated. Since the ascending phase of $x(t)$ just begins on the deactivation of the NFL, the ascending phase must be accelerated by the PFL that is still activated. This type of oscillation differs from the above two-stage oscillation whose ascending phase has no acceleration. The minimum τ_p for this new type oscillation can be determined when two feedback loops are deactivated at $t = T$, i.e.,

$$\begin{aligned} C_2 e^{-(T-t_1-\tau_p)} + \eta\alpha_n &= K, \\ C_2 e^{-(T-t_1-\tau_n)} + \eta\alpha_n &= 1, \end{aligned} \tag{C24}$$

which yields

$$\tau_p = \tau_n + \ln\frac{K-\eta\alpha_n}{1-\eta\alpha_n} > \tau_n. \tag{C25}$$

Denote $\ln\frac{K-\eta\alpha_n}{1-\eta\alpha_n}$ by ϵ_2. The above two-stage oscillation exists for $\tau_n + \epsilon_1 \leqslant \tau_p \leqslant \tau_n + \epsilon_2$. Notably, $x_{\max,1}|_{\tau_p=\tau_n+\epsilon_1} = x_{\max,2}|_{\tau_p=\tau_n+\epsilon_1}$. With $\frac{dx_{\max,1}}{d\tau_p} < 0$, $x_{\max,1} \geqslant x_{\max,2}$. For larger τ_p, i.e., $\tau_p \in (\tau_n + \epsilon_2, +\infty)$, it is impossible to analytically calculate $x(t)$, but it can be inferred from that for $\tau_p \in [0, \tau_n + \epsilon_2]$ due to the recurrence of periodic solutions.

3. $\tau_p < 0$

For $\tau_p < 0$, the PFL can be activated in advance compared with the case of $\tau_p = 0$. For a small $|\tau_p|$, $x(t)$ still undergoes three stages in one period, so the kinetic equations are the same as Eqs. (C5)–(C7). The conditions for the undetermined parameters are

$$\begin{aligned} C_1 e^{-t_1} + \eta &= C_2 + \eta\alpha_p, \\ C_2 e^{-(t_2-t_1)} + \eta\alpha_p &= C_3 + \eta\alpha_n, \\ C_3 e^{-(T-t_2)} + \eta\alpha_n &= C_1 + \eta, \\ C_1 e^{-(t_2-\tau_n)} + \eta &= 1, \\ C_2 e^{\tau_p} + \eta\alpha_p &= K, \\ C_3 e^{-(T-t_2-\tau_n)} + \eta\alpha_n &= 1. \end{aligned} \tag{C26}$$

Six parameters can be solved subsequently:

$$\begin{aligned} C_1 &= e^{-\tau_n}(1-\eta\alpha_n) - \eta(1-\alpha_n) < 0, \\ C_2 &= e^{-\tau_p}(K-\eta\alpha_p) < 0, \\ t_1 &= \ln\frac{C_1}{C_2+\eta(\alpha_p-1)}, \\ t_2 &= \tau_n + \ln\frac{C_1}{1-\eta}, \\ C_3 &= C_2 e^{-(t_2-t_1)} + \eta(\alpha_p-\alpha_n) > 0, \\ T &= t_2 + \ln\frac{C_3}{C_1+\eta(1-\alpha_n)}. \end{aligned} \tag{C27}$$

We have

$$\begin{aligned} x_{\min} &= C_1+\eta = e^{-\tau_n}(1-\eta\alpha_n)+\eta\alpha_n, \\ x_{\max,\tau_p<0} &= C_3+\eta\alpha_n \\ &= \frac{e^{-(\tau_n+\tau_p)}(K-\eta\alpha_p)(1-\eta)}{e^{-\tau_p}(K-\eta\alpha_p)+\eta(\alpha_p-1)} + \eta\alpha_p. \end{aligned} \tag{C28}$$

It can be easily verified that $x_{\max,\tau_p<0}$ is larger than $x_{\max,1}$ and $x_{\max,2}$.

APPENDIX D: STOCHASTIC SIMULATION METHOD

Here we extend the original Gillespie method [48] to simulate the stochastic dynamics of the simplified model. Given the cellular volume Ω, the number of X is $N = X\Omega = xK_n\Omega$, where x is the dimensionless concentration of X and K_n is the Michaelis constant. Suppose the current time point is t_0 and the number of X at t_0 is N_{t_0}. The propensity function (the firing rate for the reaction) of the production reaction at t, $a_1(t) = a_1(N_{t-\tau_p}, N_{t-\tau_n})$, depends on the states of the system at $t-\tau_p$ and $t-\tau_n$. The propensity function of the degradation, $a_2(t) = a_2(N_t)$, is determined by the current state. Thus, the sum of propensity function, $a(t) = a_1(t) + a_2(t)$, depends on the states of the system at three time points. Since the number of X is discrete, $a(t)$ keeps constant if no changes happen in the system states at those three time points, i.e., N_t, $N_{t-\tau_p}$, and $N_{t-\tau_n}$. Denote by $t_0 < t_1 < \cdots < t_i < \ldots$ $(i = 1,2,\ldots)$ the time points where any changes occur in the above three variables. For $t_i < t < t_{i+1}$, the waiting time τ for either of reactions to fire obeys the distribution

$$\begin{aligned} &P_i(\tau > t - t_0) \\ &\quad = e^{-a(t_0)(t_1-t_0)-a(t_1)(t_2-t_1)-\cdots-a(t_{i-1})(t_i-t_{i-1})-a(t_i)(t-t_i)}. \end{aligned} \tag{D1}$$

In each step of simulation, we sample two random numbers r_1 and r_2, which are both uniformly distributed in $[0,1]$. There must be an i such that $P_i(\tau > t - t_0) = r_1$ can have a positive solution of t. With this t, we obtain the waiting time $\tau = t - t_0$. Then, if $r_2 < a_1/a$, the production reaction fires; otherwise, the degradation reaction fires.

[1] N. A. Cookson, L. S. Tsimring, and J. Hasty, FEBS Lett. **583**, 3931 (2009).
[2] H. Zhu and Y. Mao, Sci. Rep. **5**, 14627 (2015).
[3] B. Novák and J. J. Tyson, Nat. Rev. Mol. Cell Biol. **9**, 981 (2008).
[4] M. B. Elowitz and S. Leibler, Nature **403**, 335 (2000).
[5] J. Stricker, S. Cookson, M. R. Bennett, W. H. Mather, L. S. Tsimring, and J. Hasty, Nature **456**, 516 (2008).
[6] N. Barkai and S. Leibler, Nature **403**, 267 (2000).
[7] W. Mather, M. R. Bennett, J. Hasty, and L. S. Tsimring, Phys. Rev. Lett. **102**, 068105 (2009).
[8] B. Ananthasubramaniam and H. Herzel, PLoS ONE **9**, e104761 (2014).
[9] J. Srividhya, M. S. Gopinathan, and S. Schnell, Biophys. Chem. **125**, 286 (2007).
[10] L. Glass, A. Beuter, and D. Larocque, Math. Biosci. **90**, 111 (1988).
[11] Y. Suzuki, M. Lu, E. Ben-Jacob, and J. N. Onuchic, Sci. Rep. **6**, 21037 (2016).
[12] D. V. Ramana Reddy, A. Sen, and G. L. Johnston, Phys. Rev. Lett. **80**, 5109 (1998).
[13] T. Y. Tsai, Y. S. Choi, W. Ma, J. R. Pomerening, C. Tang, and J. E. Ferrell, Jr., Science **321**, 126 (2008).
[14] H. Song, P. Smolen, E. Av-Ron, D. A. Baxter, and J. H. Byrne, Biophys. J. **92**, 3407 (2007).
[15] K. Lee, J. J. Loros, and J. C. Dunlap, Science **289**, 107 (2000).
[16] S. A. Cyran, A. M. Buchsbaum, K. L. Reddy, M. C. Lin, N. R. Glossop, P. E. Hardin, M. W. Young, R. V. Storti, and J. Blau, Cell **112**, 329 (2003).
[17] T. K. Sato, S. Panda, L. J. Miraglia, T. M. Reyes, R. D. Rudic, P. McNamara, K. A. Naik, G. A. FitzGerald, S. A. Kay, and J. B. Hogenesch, Neuron **43**, 527 (2004).
[18] T. Schafmeier, K. Káldi, A. Diernfellner, C. Mohr, and M. Brunner, Genes Dev. **20**, 297 (2006).
[19] M. Gallego and D. M. Virshup, Nat. Rev. Mol. Cell Biol. **8**, 139 (2007).
[20] M. Ukai-Tadenuma, R. G. Yamada, H. Xu, J. A. Ripperger, A. C. Liu, and H. R. Ueda, Cell **144**, 268 (2011).
[21] J. Yan, G. Shi, Z. Zhang, X. Wu, Z. Liu, L. Xing, Z. Qu, Z. Dong, L. Yang, and Y. Xu, Nucleic Acids Res. **42**, 10278 (2014).
[22] J. Hasty, F. Isaacs, M. Dolnik, D. McMillen, and J. J. Collins, Chaos **11**, 207 (2001).
[23] J. Hasty, M. Dolnik, V. Rottschafer, and J. J. Collins, Phys. Rev. Lett. **88**, 148101 (2002).
[24] X.-J. Tian, X.-P. Zhang, F. Liu, and W. Wang, Phys. Rev. E **80**, 011926 (2009).
[25] A. Tiwari and O. A. Igoshin, Phys. Biol. **9**, 055003 (2012).
[26] H. Ge, H. Qian, and X. S. Xie, Phys. Rev. Lett. **114**, 078101 (2015).
[27] B. Huang, Y. Xia, F. Liu, and W. Wang, Sci. Rep. **6**, 28096 (2016).

[28] J. E. Ferrell, Jr., J. R. Pomerening, S. Y. Kim, N. B. Trunnell, W. Xiong, C. Y. Huang, and E. M. Machleder, FEBS Lett. **583**, 3999 (2009).
[29] T. S. Gardner, C. R. Cantor, and J. J. Collins, Nature **403**, 339 (2000).
[30] H. Fazelinia, R. Sipahi, and N. Olgac, IEEE T. Automat. Contr. **52**, 799 (2007).
[31] S. Yanchuk and P. Perlikowski, Phys. Rev. E **79**, 046221 (2009).
[32] D. Bratsun, D. Volfson, L. S. Tsimring, and J. Hasty, Proc. Natl. Acad. Sci. USA **102**, 14593 (2005).
[33] M. Barrio, K. Burrage, A. Leier, and T. Tian, PLoS Comput. Biol. **2**, e117 (2006).
[34] D. F. Anderson, J. Chem. Phys. **127**, 214107 (2007).
[35] X. Cai, J. Chem. Phys. **126**, 124108 (2007).
[36] A. Leier, T. T. Marquez-Lago, and K. Burrage, J. Chem. Phys. **128**, 205107 (2008).
[37] M. R. Atkinson, M. A. Savageau, J. T. Myers, and A. J. Ninfa, Cell **113**, 597 (2003).
[38] R. Guantes and J. F. Poyatos, PLoS Comput. Biol. **2**, e30 (2006).
[39] M. Tigges, T. T. Marquez-Lago, J. Stelling, and M. Fussenegger, Nature **457**, 309 (2009).
[40] O. Purcell, N. J. Savery, C. S. Grierson, and M. di Bernardo, J. R. Soc. Interface **7**, 1503 (2010).
[41] J. Diao, D. A. Charlebois, D. Nevozhay, Z. Bódi, C. Pál, and G. Balázsi, ACS Synth. Biol. **5**, 619 (2016).
[42] K. Sriram and M. S. Gopinathan, J. Theor. Biol. **231**, 23 (2004).
[43] J. C. Leloup and A. Goldbeter, Proc. Natl. Acad. Sci. USA **100**, 7051 (2003).
[44] A. Relógio, P. O. Westermark, T. Wallach, K. Schellenberg, A. Kramer, and H. Herzel, PLoS Comput. Biol. **7**, e1002309 (2011).
[45] T. Danino, O. Mondragon-Palomino, L. Tsimring, and J. Hasty, Nature **463**, 326 (2010).
[46] A. Prindle, J. Selimkhanov, H. Li, I. Razinkov, L. S. Tsimring, and J. Hasty, Nature **508**, 387 (2014).
[47] W. Mather, J. Hasty, and L. S. Tsimring, Phys. Rev. Lett. **113**, 128102 (2014).
[48] D. T. Gillespie, J. Comput. Phys. **22**, 403 (1976).